

Boosted top quark inspired leptoquark searches at the muon collider

Arvind Bhaskar^{1,*} and Manimala Mitra^{1,2,†}

¹*Institute of Physics, Bhubaneswar, Sachivalaya Marg, Sainik School, Bhubaneswar 751005, India*

²*Homi Bhabha National Institute, Training School Complex, Anushakti Nagar, Mumbai 400094, India*

(Dated: September 26, 2024)

The proposed muon collider presents a promising avenue to explore various classes of beyond the Standard Model (BSM) particles. In this paper, we investigate the discovery prospects of the scalar leptoquark (LQ) S_1 at a muon collider. We consider two benchmark center-of-mass (C.O.M.) energy scenarios: 5 TeV and 10 TeV. We assume that the LQ decays into a top quark and a muon. The collider analysis for an LQ decaying into a top quark is distinct from that of lighter quarks. A TeV-scale LQ decaying into a top quark can produce an exotic, boosted fat-jet signature. In addition to the usual searches based on pair production of LQs, we also examine the single production mode, which depends on the $S_1 t \mu$ coupling. We demonstrate that systematically combining the pair and single production modes significantly enhances the discovery potential of the LQ at the muon collider. Our signal topology includes at least one hadronically decaying top fat-jet and two oppositely charged muons, thereby enabling the incorporation of the single production mode. We show that even with single production alone, it is possible to probe LQs as heavy as 4.5 TeV (9.0 TeV) in the 5 TeV (10 TeV) C.O.M. scenario for $\mathcal{O}(1)$ couplings.

I. INTRODUCTION

The experimental search for the particle spectrum of standard model (SM) culminated with the discovery of the Higgs boson in 2012 at the large hadron collider (LHC). Despite its tremendous success, the Standard Model (SM) remains an incomplete theory. Although there has been no direct experimental evidence of new physics at colliders, hints of physics beyond the Standard Model (BSM) have emerged in various low-energy experiments. For instance, the measurement of the anomalous magnetic moment of the muon ($(g-2)_\mu$) throws a discrepancy of $\approx 4\sigma$ between the SM calculated value and the experimental observation at Fermilab [1–4]. Many BSM models have been proposed to explain these low energy experimental anomalies. Leptoquarks (LQs) are one of the promising class of particles to explain such anomalies. LQs are color triplet and electromagnetically charged scalar and vector bosons. They can exist as a weak singlet, doublet or triplet. LQs have been explored extensively in literature [5–58], but mostly at hadron colliders. LQs are color triplets scalar or vector bosons and carry an electromagnetic charge. They appear in many BSM theories such Pati-Salam models [59], SU(5) grand unified theories (GUTs) [60], models with quark and lepton compositeness [61], R-parity violating supersymmetric models [62]. Since, they possess both baryon and lepton numbers, they can combine with quarks and leptons simultaneously. LQs can also play a role in other BSM scenarios such as the production of right handed neutrinos [25, 38, 63, 64], Higgs physics [56, 65–67], dark matter [68, 69]. In our previous works [70–72], we investigated the exotic signature of a LQ decaying to a top quark and a lepton at the high luminosity LHC (HL-LHC). The ATLAS collaboration has recently published their results of the search for scalar and vector LQs at $\sqrt{13}$ TeV with an integrated luminosity of 139 fb^{-1} [73]. ATLAS has searched for LQs (scalar and vector) decaying to top quarks and light leptons (e, μ). They have excluded a sLQ of mass 1.58 (1.59) TeV decaying to a top

quark and electron (muon) with 100% branching ratio (BR) with 95% confidence limits (C.L). Similarly, the exclusion limits on its vector counterpart decaying to the same final states are 1.67 TeV in the minimal coupling scenario and 1.95 TeV in the Yang-Mills scenario. The discovery reach for the same final state at the HL-LHC is only about 1.7 TeV [70], which motivates to explore the sLQ signal at a lepton collider, where the entire center of mass (C.O.M) energy is accessible for resonant production of particles. In this work, we study the discovery prospects of scalar LQs (sLQs) decaying to similar final state at the muon collider [74, 75]. There are some existing works on the search for LQs at the proposed muon collider [76, 77]. A muon collider has certain advantages over a hadron collider. Being a fundamental particle, the muon has the entire C.O.M energy available for collision. It offers high precision measurement of the SM processes. Additionally, the heavier mass of the muon results in reduced energy loss due to synchrotron radiation, allowing for higher energy and luminosity. A muon collider can generate interactions over a range of partonic C.O.M energy \sqrt{s} . In this paper, we investigate the discovery reach of the sLQ decaying to a top quark and a muon at the proposed muon collider. We consider the contributions from both the resonant pair and single production of sLQs in our analysis. The single production contribution is included because at higher masses, its contribution falls less rapidly as compared to the pair production process due to less phase space suppression. We also discuss about an additional nonresonant mode of LQ production leading to the same final states. We systematically incorporate all the relevant production modes of the sLQ that contribute to the desired final state involving a pair of top quarks and dimuons. We consider the hadronic decay of the top quark which forms an exotic boosted fatjet signature. To perform the analysis, we consider two benchmark C.O.M energies– 5 TeV and 10 TeV and their corresponding integrated luminosities at 3 ab^{-1} and 10 ab^{-1} respectively. We find that a muon collider with the above mentioned C.O.M energy outperforms the discovery reach of a sLQ decaying to a similar final state at the HL-LHC. We highlight its capabilities in probing higher energy scales and achieving greater precision in the study of new physics.

The paper is organised as follows: we introduce the sLQ

* arvind.bhaskar@iopb.res.in

† manimala@iopb.res.in

model in section II. We discuss the decay widths and branching ratios in section III, and explain the search strategy in section IV. Finally, we present our results and conclude in section V.

II. THEORETICAL SET UP

In this paper, we consider a weakly singlet scalar leptoquark $S_1 = (\mathbf{3}, 1, 1/3)$. Following the notation of Ref. [78], the interaction terms of the S_1 Lagrangian can be written as follows:

$$\mathcal{L} \supset y_{1ij}^{LL} \bar{Q}_L^C S_1^i \sigma^2 L_L^j + y_{1ij}^{RR} \bar{u}_R^C S_1^i \ell_R^j + \text{H.c.}, \quad (1)$$

where u_R and ℓ_R are a SM right-handed up-type quark and a charged lepton, respectively. Q_L and L_L are the SM left-handed quark and lepton doublets, respectively. The superscript C denotes charge conjugation and σ^2 is the second Pauli matrix. The generation indices are denoted by $i, j = \{1, 2, 3\}$. The color indices are suppressed. We write the neutrinos collectively as ν since the LHC is neutrino flavours-blind. We focus on S_1 , that exclusively interacts with a second generation lepton and a third generation quark. Hence, the above Lagrangian simplifies to the following terms,

$$\mathcal{L} \supset y_{132}^{LL} \left(-\bar{\ell}_L^C \nu_\mu + \bar{\ell}_L^C \mu_L^j \right) S_1 + y_{132}^{RR} \bar{t}_R^C \mu_R^j S_1 + \text{H.c.} \quad (2)$$

Note that, in the above the superscript LL/RR on the coupling y_1 represents the chirality of the μ and t . In the rest of the work, we shall use y_1 as a generalized notation for our new coupling and specify the chirality when required.

III. DECAY WIDTH AND BRANCHING RATIOS

If we consider only a nonzero y_{132}^{LL} in Eq. (2), then S_1 can decay to a top quark and a muon and it can also decay to b quark and a neutrino with a BR $\approx 50\%$. Whereas, if one considers only the y_{132}^{RR} to be nonzero then the S_1 decays to a top quark and a muon with 100% BR. We show the expressions of the decay widths for S_1 sLQ as a function of its mass M_{S_1} and new coupling y_1 .

$$\Gamma(S_1 \rightarrow t\mu) = \frac{(M_{S_1}^2 - m_t^2)^2 [(y_{132}^{LL})^2 + (y_{132}^{RR})^2]}{16\pi M_{S_1}^2} \quad (3)$$

$$\Gamma(S_1 \rightarrow b\nu) = \frac{(M_{S_1}^2 - m_b^2)^2 (y_{132}^{LL})^2}{16\pi M_{S_1}^2} \quad (4)$$

IV. SEARCH STRATEGY OF SLQ AT THE MUON COLLIDER

We use the FeynRules [79] software package to encode the Lagrangian mentioned in Eqs. (2) to generate the universal Feynman output (UFO) model file. We generate the signal and background events using MadGraph5aMC@NLO-v3.5.3 [80] at the leading order (LO). The generated signal and background events are passed through Pythia8 [81] for showering and hadronization. For simulating the detector effects we use Delphes3 [82] with Delphes ILLD card. We cluster the fatjets coming from the decay of top quarks using Cambridge-Aachen [83] clustering algorithm (with $R = 1.5$) in FastJet [84].

A. Production at the Muon collider

The LQs can be produced resonantly as a pair or singly along with a top quark and a muon. In Figure. 1(a), we show the representative Feynman diagram for pair production of S_1 , mediated by a Z boson or a photon. This contribution doesn't depend on the new coupling y_1 . Figure. 1(b) depicts the S_1 pair production via a t -channel top quark exchange. The cross-section contribution from this t -channel diagram is proportional to the fourth power of the new coupling constant $-y_1^4$. Additionally, there is a destructive interference between these two diagrams. The cross section from this interference term scales as y_1^2 . Once produced, the sLQ decays to either a top quark and a charged lepton or a bottom quark and a neutrino depending on the chirality of the yukawa coupling y_1 , leading to the following final states.

$$\mu^- \mu^+ \rightarrow \{ S_1 \bar{S}_1 \rightarrow (t\mu)(t\mu) / (b\nu)(b\nu) \}. \quad (5)$$

For the single production of LQs (see Fig. 1(c)), the cross section contribution scales as y_1^2 . For single production, the subsequent decay of S_1 leads to the following final states,

$$\mu^- \mu^+ \rightarrow \left\{ \begin{array}{l} S_1 t\mu \rightarrow (t\mu)t\mu \\ S_1 t\mu \rightarrow (b\nu)t\mu \\ S_1 b\nu \rightarrow (t\mu)b\nu \\ S_1 b\nu \rightarrow (b\nu)b\nu \end{array} \right\}, \quad (6)$$

(7)

We also consider the processes such $\mu^+ \mu^- \rightarrow S_1 S_1^* \rightarrow S_1 t\mu$, that could contribute to the single production mode. In addition to these two resonant S_1 production modes leading to ditop and dimuon final state, there is an additional nonresonant production mode that leads to the same final state. In Fig. 1(d), we show the respective Feynman diagram for this process. The cross section for this t -channel exchange contribution scales as y_1^8 . For our discovery prospect studies, we ignore the contribution from this mode as the cross section is small compared to the pair and single production modes. But this mode can become important for higher LQ masses and large y_1 couplings. In this paper, we focus on the following final state signature:

$$\mu^- \mu^+ \rightarrow S_1 \bar{S}_1, S_1 t\mu \rightarrow (t\mu)(t\mu) \quad (8)$$

In Fig. 2, we have shown the cross section for the S_1 resonant (pair and single) and non-resonant production modes as a function of its mass for the choice of new couplings $y_1 = 1.0$ and C.O.M energies ($\sqrt{s} = 5, 10$ TeV). The legend mentioned in Fig. 2 is explained as follows. $lqlq$ -SM corresponds to the pair production contribution from the Feynman diagram in Fig. 1(a). $lqlq$ -NPQED corresponds to the contribution coming from the interference between the diagrams in Fig. 1(a) and Fig. 1(b). $lq\mu t$ stands for the contribution from the single production mode (Fig. 1(c) and other single production diagrams such as, $\mu^+ \mu^- \rightarrow \mu^+ \mu^-^* \rightarrow S_1 t\mu$) and $tt\mu\mu$ shows the cross section contribution from the nonresonant mode (Fig. 1(d)). In Figs 2(a) and 2(c), we show the production cross section of sLQs for couplings y_{132}^{LL} and y_{132}^{RR} , respectively at C.O.M $\sqrt{s} = 5$ TeV. Similarly in Figs. 2(b) and 2(d), we show the cross section for left handed and right handed Yukawa coupling at C.O.M $\sqrt{s} = 10$ TeV. We consider the benchmark coupling $y_{132}^{LL/RR} = 1.0$ for all of the scenarios. As stated above, once produced, we primarily consider the decay of sLQ to top quark and muon and ignore the final states containing a

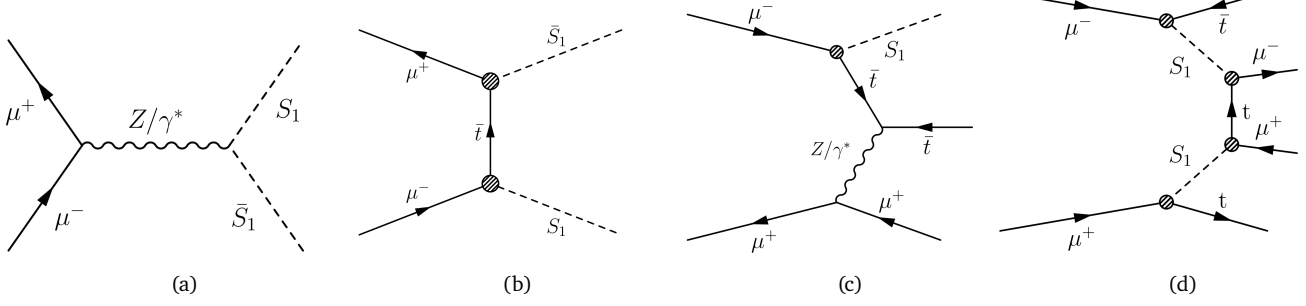


FIG. 1. We show the representative Feynman diagrams for the S_1 production at the muon collider. (a) and (b) correspond to the pair production mode. (c) shows the single production mode. (d) stands for the nonresonant production mode.

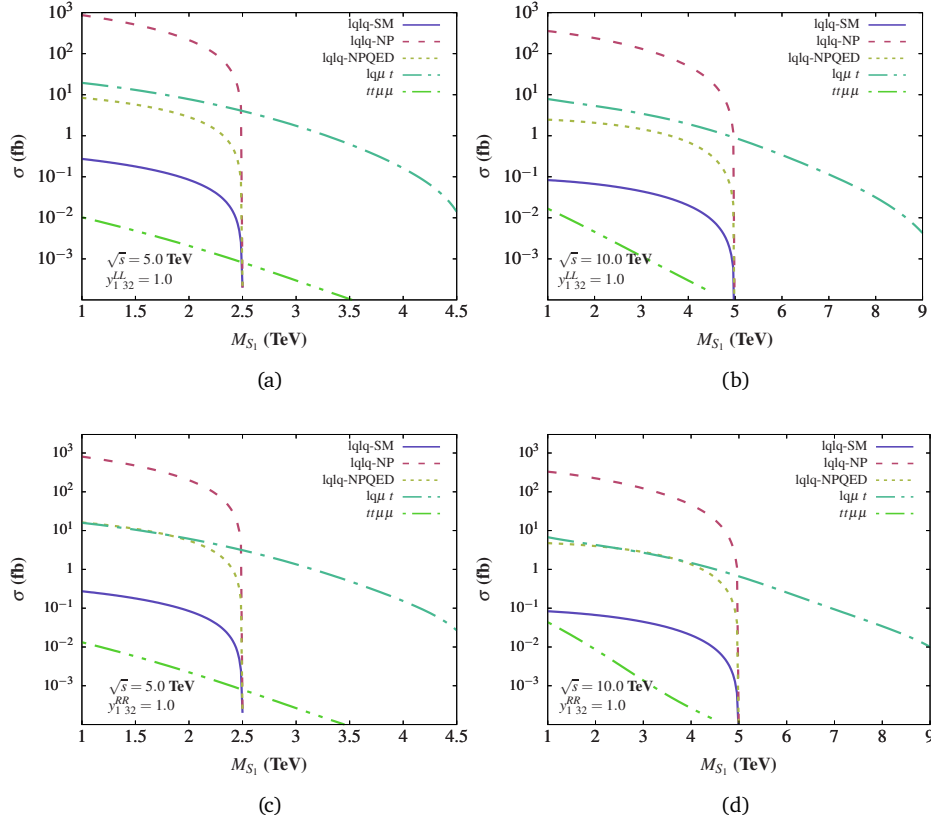


FIG. 2. The production cross section of S_1 for illustrative values of $y_{1\ 32}^{LL}$ and $y_{1\ 32}^{RR}$ at $\sqrt{s} = 5.0$ TeV [(a) and (c)] and for $y_{1\ 32}^{LL}$ and $y_{1\ 32}^{RR}$ at $\sqrt{s} = 10.0$ TeV [(b) and (d)]. We have presented the contributions from both the resonant pair and single production modes, as well as the non-resonant production mode. For all processes dependent on the Yukawa coupling y_1 , we have adopted the benchmark value of $y_1 = 1.0$.

b quark and neutrino. The top quark produced from a TeV scale sLQ will form a boosted fatjet and shall be accompanied by a high p_T muon. In the next sub-section, in defining our analysis strategy, we keep this into consideration, and therefore, we demand the presence of at least one boosted top quark forming a fatjet in the final state.

B. Signal selection and background processes

We consider at least one hadronically decaying top quark that forms a fatjet and exactly two high- p_T opposite sign

muons as our signal. The motivation for choosing such a signal is to include the contributions from the single production mode as well. We consider the hadronic decay of the top quark, as the decay of the W boson (originating from the top quark) to jets is more probable than its leptonic decay. Moreover, being a muon collider, the hadronic final state containing a high $p_T > 500$ GeV fat-jet may over-rule similar final state generated from relatively smaller SM background. We list the appropriate SM processes that can contribute as background processes in Table I, and present a brief discussion below.

1. $V + \text{jets}$: $V = W, Z$. The SM W and Z boson production plus additional jets can act as potential background processes that can lead to the desired final state.

Background processes		$\sigma(10.0)$ TeV (pb)	$\sigma(5.0)$ TeV (pb)
$V + jets$	$Z + jets$	1.34×10^{-7}	1.04×10^{-6}
	$W + jets$	0.0001915	0.001063
$VV + jets$	$WW + jets$	0.0001666	5.2×10^{-5}
$tt + jets$	–	9.9×10^{-5}	6.5×10^{-5}
$tt\mu\mu$	–	3.65×10^{-7}	8.0×10^{-7}

TABLE I. We list the dominant background processes for our analysis. These cross sections have been obtained for C.O.M energies $\sqrt{s} = 10$ TeV and $\sqrt{s} = 5$ TeV.

- $W + jets$: We generate this background by simulating the process $\mu^- \mu^+ \rightarrow W^\pm + jets$. The W decays to a muon and a neutrino. The additional jets can mimic the top-like fatjet. The second muon can come from a jet misidentified as a lepton.
 - $Z + jets$: The Z background is obtained similarly. The Z boson decays leptonically into a dimuon final state. The top-like fatjet is obtained from combining the additional jets.
2. $t\bar{t} + jets$: The ditop production is one of the dominant background processes. Here, we decay both the top quarks to muons and neutrinos. The top-like fatjet can be obtained by the additional QCD jets and the b quarks.
 3. $VV + jets$: There are two types of SM diboson processes which can serve as background.
 - $WW + jets$: Here, we generate two W bosons and decay both of them to dimuons and neutrinos in the final state. The top-like fatjet can be obtained by combining the additional QCD jets.
 - $Z\ell Z_h + jets$: Here, one of the Z decays to dimuons and the other one decays hadronically to QCD jets. Combining the hadronic decays of the Z boson with the additional QCD jets, one could reconstruct the top-like fatjet.
 4. $t\bar{t}\mu^- \mu^+$: We decay the top quarks hadronically to b quarks and W bosons. The W boson further decays to a pair of QCD jets.

For better statistics, we apply some generational level cuts on our background processes. We list the generational level cuts.

1. $p_T(\mu_1) > 80$ GeV,
2. $p_T(j_1) > 100$ GeV,
3. Invariant mass $M(\mu_1, \mu_2) > 110$ GeV (Z -mass veto),
4. $H_T > 500$ GeV.

Here j_i and μ_i denotes the i^{th} p_T -ordered jet and muon respectively. After generating events with the above generation-level cuts, we apply the following final selection criteria sequentially on the signal and the background events.

C. Discovery potential

Below, we explain the cut flow algorithm for signal selection and the list of cuts applied on the signal and background

events. We mention the cuts for the benchmark scenario $\sqrt{s} = 10$ TeV and coupling $y_1^{L_{32}} = 1.0$. Similar steps and cuts have been followed for the other benchmarks scenarios.

- Two opposite sign-muons, with atleast one muon with a high $p_T(\mu_1) > 300$ GeV and pseudorapidity $|\eta(\mu)| < 2.5$.
- Invariant mass of the lepton pair $M(\mu_1, \mu_2) > 200$ GeV.
- Atleast one b quark with a $p_T(b) > 200$ GeV.
- Atleast one top-like fatjet with mass of the fatjet, $160 < m_{fj} < 200$ GeV. Here, fj implies fatjet.
- Transverse momentum of the top-like fatjet $p_T^{fj} > 500$ GeV. Scalar sum of transverse momentum $H_T > 900$ GeV.

We calculate the statistical significance \mathcal{Z} [85] using the following formula,

$$\mathcal{Z} = \sqrt{2(N_S + N_B) \ln \left(\frac{N_S + N_B}{N_B} \right) - 2N_S}, \quad (9)$$

where N_S and N_B are the numbers of the signal and background events, respectively, surviving the selection cuts as mentioned above.

$$N_S = (\sigma_{\text{pair}} \times \epsilon_{\text{pair}} \times \beta^2 + y_1^2 \sigma_{\text{single}} \times \epsilon_{\text{single}} \times \beta) \times \mathcal{L} \quad (10)$$

$$N_B = \sigma_B \times \epsilon_B \times \mathcal{L}, \quad (11)$$

Here, we define σ_{pair} as,

$$\sigma_{\text{pair}} = \sigma_{SM} + y_1^2 \sigma_{NPQED} + y_1^4 \sigma_{NP} \quad (12)$$

where σ_{pair} is the cross section from the combined pair production mode. σ_{SM} , σ_{NP} and σ_{NPQED} are the cross sections from Feynman diagrams in the Figs. 1(a), 1(b) and the interference of the two respectively. σ_{single} is the cross section from the single production process, σ_B is the cross section of the background process, ϵ_x denotes the fraction of events surviving the cuts mentioned above, β is the appropriate BR and \mathcal{L} is the luminosity of the muon collider. ϵ_{pair} remains similar for the different pair production contributions mentioned in Eq. (12). For the benchmark scenario $\sqrt{s} = 10$ TeV, we have assumed the luminosity to be 10 ab^{-1} and for $\sqrt{s} = 5$ TeV, we have assumed the luminosity to be 3 ab^{-1} .

V. RESULTS AND CONCLUSION

In this work, we have investigated the discovery reach of the sLQ S_1 decaying to a top quark and a muon at the proposed muon collider. We systematically combine the contributions from pair and single production of S_1 in order to maximise the discovery reach. Our signal topology comprises of atleast one hadronically decaying top quark and exactly two opposite sign muons of which one must have a high p_T . We show our results in Figs. 3 and 4. In Fig. 3, we show the 5σ discovery reach contours for pair (blue dashed), single (red solid) and combined (green dashed) production modes as function of the mass of S_1 and the new coupling y_1 . These plots shows the least value of y_1 required for to observe S_1 signal with 5σ significance for a given mass. The light yellow shaded region denotes the maximum sLQ mass the muon collider can probe with 5σ significance if the coupling independent pair only mode is considered (See Fig. 1(a)). The light violet region is excluded by the LHC with 95% confidence limit (C.L) for the LQ searches

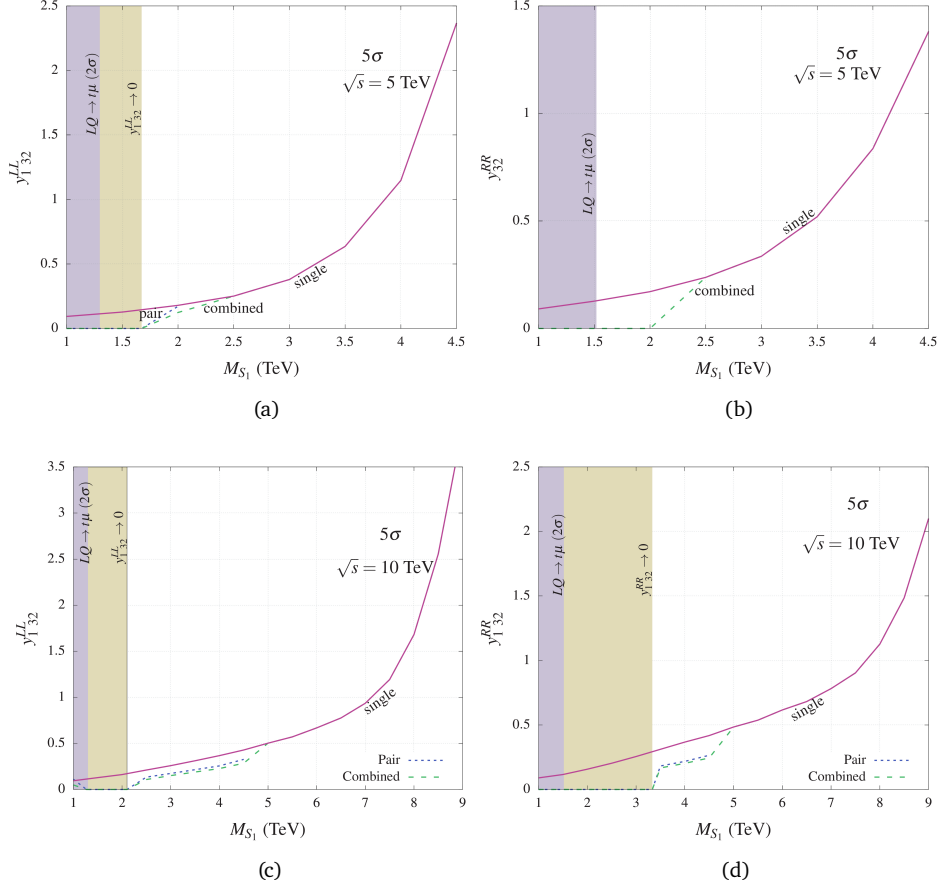


FIG. 3. The 5σ discovery reach contours as a function of the new yukawa coupling y_1 and M_{S_1} (TeV) for benchmark C.O.M energies 5.0 TeV [(a) and (b)] and 10.0 TeV [(c) and (d)]. These plots show the smallest coupling y_1 required to obtain a 5σ discovery reach for a range of S_1 mass at an integrated luminosity of 3ab^{-1} and 10ab^{-1} respectively. The yellow color shows the discovery reach if one assumes the coupling independent pair production contribution only. The violet color shows the region excluded by the LHC searches with 95% C.L.

to top quark and muon[73]. In Figs. 3(a) [3(b)], we plot the 5σ contours for the new coupling y_{132}^{LL} [y_{132}^{RR}] for the 5.0 TeV benchmark scenario. Similar plots are shown for the 10 TeV benchmark scenario in Figs. 3(c) and 3(d).

In Figs. 3(a) and 3(b), the pair production contribution ceases beyond the sLQ mass 2.0 TeV due to phase space suppression. Post 2.0 TeV, the combined mode comprises only of the single production process. In Fig. 3(a), assuming a small coupling y_1 , the muon collider can probe a LQ as heavy as 1.6 TeV (light yellow region). If we assume only the single production mode, the muon collider can probe a sLQ as heavy as 4.5 TeV with $\mathcal{O}(1)$ new coupling with 5σ significance. In Fig. 3(c) (3(d)), assuming a small coupling y_1 , the discovery reach of the sLQ goes upto 2.1(3.3) TeV. The discovery reach is higher for the right handed coupling because the branching ratio of sLQ to top quark and muon is 100% in the right handed scenario (y_{132}^{RR}). Similarly, if we assume only the single production mode, then the muon collider can probe a LQ as heavy as 9 TeV with 5σ significance, while still keeping the new couplings within perturbative limits. In Fig. 4, we show similar plots for 2σ exclusion limits. In the absence of a discovery, these plots show the maximum a sLQ can be excluded with 95% C.L. In Fig. 4(d), we can exclude a sLQ as heavy as ≈ 4.2 TeV with 95% C.L. if we consider the coupling independent pair produc-

tion search only.

These results clearly demonstrate the superiority of a muon collider over the HL-LHC [70] in probing heavier BSM particles. The projected sensitivity reach of HL-LHC for similar final state is only about 1.7 TeV at 5σ C.L [70], and hence a muon collider clearly out-performs the HL-LHC in probing sLQ. Despite following a cut-based approach for determining the discovery and exclusion, we obtained some promising yet conservative results. In our upcoming work, we plan to utilise sophisticated machine learning (ML) technique to maximise signal background separation and further enhance the discovery potential. Since a ML based approach would enhance the signal efficiency it would allow us to utilise the nonresonant production mode of the sLQ which otherwise due to its smaller cross section doesn't contribute significantly. This non-resonant production mode is suitable for probing LQs heavier than the C.O.M and for larger couplings.

ACKNOWLEDGMENTS

The authors acknowledge the use of SAMKHYA: High-Performance Computing Facility provided by the Institute of Physics (IOP), Bhubaneswar. M.M acknowledges the IPPP Diva Award research grant.

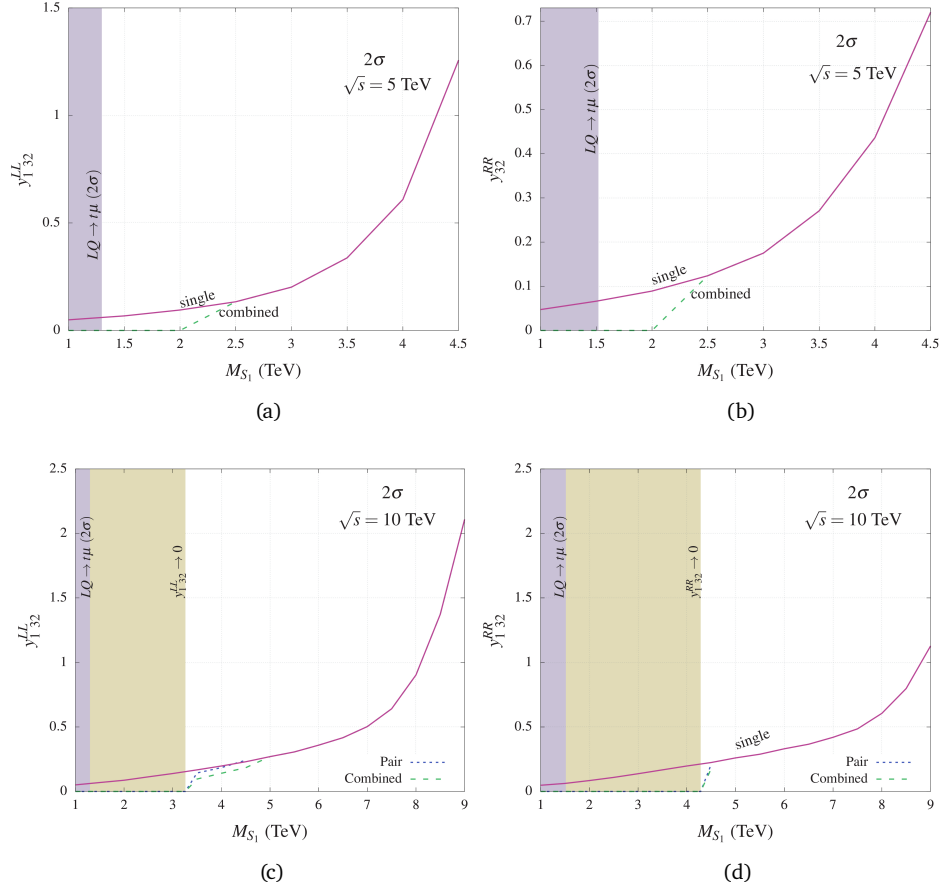


FIG. 4. The 2σ exclusion limits as a function of the new yukawa coupling y_1 and M_{S_1} (TeV) for benchmark C.O.M energies 5.0 TeV [(a) and (b)] and 10.0 TeV [(c) and (d)].

-
- [1] **Muon g-2** collaboration, G. Venanzoni, *New results from the Muon g-2 Experiment*, *PoS EPS-HEP2023* (2024) 037, [2311.08282].
 - [2] **Muon g-2** collaboration, P. Girotti, *The precision measurement of the muon $g - 2$ at Fermilab*, *Nuovo Cim. C* **47** (2024) 87.
 - [3] T. Aoyama et al., *The anomalous magnetic moment of the muon in the Standard Model*, *Phys. Rept.* **887** (2020) 1–166, [2006.04822].
 - [4] **Muon g-2** collaboration, B. Abi et al., *Measurement of the Positive Muon Anomalous Magnetic Moment to 0.46 ppm*, *Phys. Rev. Lett.* **126** (2021) 141801, [2104.03281].
 - [5] Y. Sakaki, M. Tanaka, A. Tayduganov and R. Watanabe, *Testing leptoquark models in $\bar{B} \rightarrow D^{(*)}\tau\bar{\nu}$* , *Phys. Rev. D* **88** (2013) 094012, [1309.0301].
 - [6] R. Mohanta, *Effect of scalar leptoquarks on the rare decays of B_s meson*, *Phys. Rev. D* **89** (2014) 014020, [1310.0713].
 - [7] S. Sahoo and R. Mohanta, *Scalar leptoquarks and the rare B meson decays*, *Phys. Rev. D* **91** (2015) 094019, [1501.05193].
 - [8] U. K. Dey and S. Mohanty, *Constraints on Leptoquark Models from IceCube Data*, *JHEP* **04** (2016) 187, [1505.01037].
 - [9] T. Mandal, S. Mitra and S. Seth, *Pair Production of Scalar Leptoquarks at the LHC to NLO Parton Shower Accuracy*, *Phys. Rev. D* **93** (2016) 035018, [1506.07369].
 - [10] M. Freytsis, Z. Ligeti and J. T. Ruderman, *Flavor models for $\bar{B} \rightarrow D^{(*)}\tau\bar{\nu}$* , *Phys. Rev. D* **92** (2015) 054018, [1506.08896].
 - [11] S. Sahoo and R. Mohanta, *Study of the rare semileptonic decays $B_d^0 \rightarrow K^*l^+l^-$ in scalar leptoquark model*, *Phys. Rev. D* **93** (2016) 034018, [1507.02070].
 - [12] S. Sahoo and R. Mohanta, *Leptoquark effects on $b \rightarrow s\nu\bar{\nu}$ and $B \rightarrow Kl^+l^-$ decay processes*, *New J. Phys.* **18** (2016) 013032, [1509.06248].
 - [13] U. Aydemir, *SO(10) grand unification in light of recent LHC searches and colored scalars at the TeV-scale*, *Int. J. Mod. Phys. A* **31** (2016) 1650034, [1512.00568].
 - [14] S. Sahoo and R. Mohanta, *Lepton flavor violating B meson decays via a scalar leptoquark*, *Phys. Rev. D* **93** (2016) 114001, [1512.04657].
 - [15] U. Aydemir and T. Mandal, *LHC probes of TeV-scale scalars in SO(10) grand unification*, *Adv. High Energy Phys.* **2017** (2017) 7498795, [1601.06761].
 - [16] D. Das, C. Hati, G. Kumar and N. Mahajan, *Towards a unified explanation of $R_{D^{(*)}}$, R_K and $(g - 2)_\mu$ anomalies in a left-right model with leptoquarks*, *Phys. Rev. D* **94** (2016) 055034, [1605.06313].
 - [17] S. Sahoo and R. Mohanta, *Effects of scalar leptoquark on semileptonic Λ_b decays*, *New J. Phys.* **18** (2016) 093051, [1607.04449].

- [18] D. Bečirević, N. Košnik, O. Sumensari and R. Zukanovich Funchal, *Palatable Leptoquark Scenarios for Lepton Flavor Violation in Exclusive $b \rightarrow s\ell_1\ell_2$ modes*, *JHEP* **11** (2016) 035, [[1608.07583](#)].
- [19] P. Bandyopadhyay and R. Mandal, *Vacuum stability in an extended standard model with a leptoquark*, *Phys. Rev. D* **95** (2017) 035007, [[1609.03561](#)].
- [20] S. Sahoo, R. Mohanta and A. K. Giri, *Explaining the R_K and $R_{D^{(*)}}$ anomalies with vector leptoquarks*, *Phys. Rev. D* **95** (2017) 035027, [[1609.04367](#)].
- [21] D. A. Faroughy, A. Greljo and J. F. Kamenik, *Confronting lepton flavor universality violation in B decays with high- p_T tau lepton searches at LHC*, *Phys. Lett. B* **764** (2017) 126–134, [[1609.07138](#)].
- [22] G. Hiller, D. Loose and K. Schönwald, *Leptoquark Flavor Patterns & B Decay Anomalies*, *JHEP* **12** (2016) 027, [[1609.08895](#)].
- [23] B. Bhattacharya, A. Datta, J.-P. Guévin, D. London and R. Watanabe, *Simultaneous Explanation of the R_K and $R_{D^{(*)}}$ Puzzles: a Model Analysis*, *JHEP* **01** (2017) 015, [[1609.09078](#)].
- [24] M. Duraisamy, S. Sahoo and R. Mohanta, *Rare semileptonic $B \rightarrow K(\pi)l_i^-l_j^+$ decay in a vector leptoquark model*, *Phys. Rev. D* **95** (2017) 035022, [[1610.00902](#)].
- [25] D. Das, K. Ghosh, M. Mitra and S. Mondal, *Probing sterile neutrinos in the framework of inverse seesaw mechanism through leptoquark productions*, *Phys. Rev. D* **97** (2018) 015024, [[1708.06206](#)].
- [26] N. Assad, B. Fornal and B. Grinstein, *Baryon Number and Lepton Universality Violation in Leptoquark and Diquark Models*, *Phys. Lett. B* **777** (2018) 324–331, [[1708.06350](#)].
- [27] U. K. Dey, D. Kar, M. Mitra, M. Spannowsky and A. C. Vincent, *Searching for Leptoquarks at IceCube and the LHC*, *Phys. Rev. D* **98** (2018) 035014, [[1709.02009](#)].
- [28] A. Biswas, D. K. Ghosh, S. K. Patra and A. Shaw, *$b \rightarrow c\ell\nu$ anomalies in light of extended scalar sectors*, *Int. J. Mod. Phys. A* **34** (2019) 1950112, [[1801.03375](#)].
- [29] P. Bandyopadhyay and R. Mandal, *Revisiting scalar leptoquark at the LHC*, *Eur. Phys. J. C* **78** (2018) 491, [[1801.04253](#)].
- [30] U. Aydemir, D. Minic, C. Sun and T. Takeuchi, *B -decay anomalies and scalar leptoquarks in unified Pati-Salam models from noncommutative geometry*, *JHEP* **09** (2018) 117, [[1804.05844](#)].
- [31] J. Kumar, D. London and R. Watanabe, *Combined Explanations of the $b \rightarrow s\mu^+\mu^-$ and $b \rightarrow c\tau^-\bar{\nu}$ Anomalies: a General Model Analysis*, *Phys. Rev. D* **99** (2019) 015007, [[1806.07403](#)].
- [32] A. Angelescu, D. Bečirević, D. Faroughy and O. Sumensari, *Closing the window on single leptoquark solutions to the B -physics anomalies*, *JHEP* **10** (2018) 183, [[1808.08179](#)].
- [33] T. Mandal, S. Mitra and S. Raz, *$R_{D^{(*)}}$ motivated S_1 leptoquark scenarios: Impact of interference on the exclusion limits from LHC data*, *Phys. Rev. D* **99** (2019) 055028, [[1811.03561](#)].
- [34] S. Iguro, T. Kitahara, Y. Omura, R. Watanabe and K. Yamamoto, *D^* polarization vs. $R_{D^{(*)}}$ anomalies in the leptoquark models*, *JHEP* **02** (2019) 194, [[1811.08899](#)].
- [35] J. Aebischer, A. Crivellin and C. Greub, *QCD improved matching for semileptonic B decays with leptoquarks*, *Phys. Rev. D* **99** (2019) 055002, [[1811.08907](#)].
- [36] S. Bar-Shalom, J. Cohen, A. Soni and J. Wudka, *Phenomenology of TeV-scale scalar Leptoquarks in the EFT*, *Phys. Rev. D* **100** (2019) 055020, [[1812.03178](#)].
- [37] T. J. Kim, P. Ko, J. Li, J. Park and P. Wu, *Correlation between $R_{D^{(*)}}$ and top quark FCNC decays in leptoquark models*, *JHEP* **07** (2019) 025, [[1812.08484](#)].
- [38] S. Mandal, M. Mitra and N. Sinha, *Probing leptoquarks and heavy neutrinos at the LHeC*, *Phys. Rev. D* **98** (2018) 095004, [[1807.06455](#)].
- [39] A. Biswas, D. Kumar Ghosh, N. Ghosh, A. Shaw and A. K. Swain, *Collider signature of U_1 Leptoquark and constraints from $b \rightarrow c$ observables*, *J. Phys. G* **47** (2020) 045005, [[1808.04169](#)].
- [40] R. Mandal, *Fermionic dark matter in leptoquark portal*, *Eur. Phys. J. C* **78** (2018) 726, [[1808.07844](#)].
- [41] A. Biswas, A. Shaw and A. K. Swain, *Collider signature of V_2 Leptoquark with $b \rightarrow s$ flavour observables*, *LHEP* **2** (2019) 126, [[1811.08887](#)].
- [42] J. Roy, *Probing leptoquark chirality via top polarization at the Colliders*, *1811.12058*.
- [43] S. Sahoo and R. Mohanta, *Impact of vector leptoquark on $\bar{B} \rightarrow \bar{K}^*l^+l^-$ anomalies*, *J. Phys. G* **45** (2018) 085003, [[1806.01048](#)].
- [44] A. Crivellin, C. Greub, D. Müller and F. Saturnino, *Importance of Loop Effects in Explaining the Accumulated Evidence for New Physics in B Decays with a Vector Leptoquark*, *Phys. Rev. Lett.* **122** (2019) 011805, [[1807.02068](#)].
- [45] S. Balaji, R. Foot and M. A. Schmidt, *Chiral $SU(4)$ explanation of the $b \rightarrow s$ anomalies*, *Phys. Rev. D* **99** (2019) 015029, [[1809.07562](#)].
- [46] B. Fornal, S. A. Gadam and B. Grinstein, *Left-Right $SU(4)$ Vector Leptoquark Model for Flavor Anomalies*, *Phys. Rev. D* **99** (2019) 055025, [[1812.01603](#)].
- [47] E. Alvarez and M. Szewc, *Nonresonant leptoquark with multigeneration couplings for $\mu\mu jj$ and $\mu\nu jj$ at the LHC*, *Phys. Rev. D* **99** (2019) 095004, [[1811.05944](#)].
- [48] R. Mandal and A. Pich, *Constraints on scalar leptoquarks from lepton and kaon physics*, *JHEP* **12** (2019) 089, [[1908.11155](#)].
- [49] W.-S. Hou, T. Modak and G.-G. Wong, *Scalar leptoquark effects on $B \rightarrow \mu\bar{\nu}$ decay*, *Eur. Phys. J. C* **79** (2019) 964, [[1909.00403](#)].
- [50] R. Padhan, S. Mandal, M. Mitra and N. Sinha, *Signatures of \tilde{R}_2 class of Leptoquarks at the upcoming ep colliders*, *1912.07236*.
- [51] U. Aydemir, T. Mandal and S. Mitra, *Addressing the $R_{D^{(*)}}$ anomalies with an S_1 leptoquark from $SO(10)$ grand unification*, *Phys. Rev. D* **101** (2020) 015011, [[1902.08108](#)].
- [52] B. Allanach, T. Corbett and M. Madigan, *Sensitivity of Future Hadron Colliders to Leptoquark Pair Production in the Di-Muon Di-Jets Channel*, *Eur. Phys. J. C* **80** (2020) 170, [[1911.04455](#)].
- [53] J. Zhang, C.-X. Yue, C.-H. Li and S. Yang, *Constraints on scalar and vector leptoquarks from the LHC Higgs data*, *1905.04074*.
- [54] C. Cornella, J. Fuentes-Martin and G. Isidori, *Revisiting the vector leptoquark explanation of the B -physics anomalies*, *JHEP* **07** (2019) 168, [[1903.11517](#)].
- [55] M. J. Baker, J. Fuentes-Martin, G. Isidori and M. König, *High- p_T signatures in vector-leptoquark models*, *Eur. Phys. J. C* **79** (2019) 334, [[1901.10480](#)].
- [56] A. Bhaskar, D. Das, B. De and S. Mitra, *Enhancement of Higgs Production Through Leptoquarks at the LHC*, *2002.12571*.

- [57] P. Bandyopadhyay, S. Dutta and A. Karan, *Investigating the Production of Leptoquarks by Means of Zeros of Amplitude at Photon Electron Collider*, [2003.11751](#).
- [58] J. Blumlein, E. Boos and A. Kryukov, *Leptoquark pair production in hadronic interactions*, *Z. Phys. C* **76** (1997) 137–153, [[hep-ph/9610408](#)].
- [59] J. C. Pati and A. Salam, *Lepton Number as the Fourth Color*, *Phys. Rev. D* **10** (1974) 275–289. [Erratum: *Phys. Rev. D* **11**, 703 (1975)].
- [60] H. Georgi and S. L. Glashow, *Unity of All Elementary Particle Forces*, *Phys. Rev. Lett.* **32** (1974) 438–441.
- [61] B. Schrempp and F. Schrempp, *Light Leptoquarks*, *Phys. Lett. B* **153** (1985) 101–107.
- [62] R. Barbier et al., *R-parity violating supersymmetry*, *Phys. Rept.* **420** (2005) 1–202, [[hep-ph/0406039](#)].
- [63] J. L. Evans and N. Nagata, *Signatures of Leptoquarks at the LHC and Right-handed Neutrinos*, *Phys. Rev. D* **92** (2015) 015022, [[1505.00513](#)].
- [64] A. Bhaskar, Y. Chaurasia, K. Deka, T. Mandal, S. Mitra and A. Mukherjee, *Right-handed neutrino pair production via second-generation leptoquarks*, *Phys. Lett. B* **843** (2023) 138039, [[2301.11889](#)].
- [65] P. Agrawal and U. Mahanta, *Leptoquark contribution to the Higgs boson production at the CERN LHC collider*, *Phys. Rev. D* **61** (2000) 077701, [[hep-ph/9911497](#)].
- [66] P. Fileviez Perez, E. Golias and A. D. Plascencia, *Probing quark-lepton unification with leptoquark and Higgs boson decays*, *Phys. Rev. D* **105** (2022) 075011, [[2107.06895](#)].
- [67] A. Bhaskar, D. Das, B. De, S. Mitra, A. K. Nayak and C. Neeraj, *Leptoquark-assisted singlet-mediated di-Higgs production at the LHC*, *Phys. Lett. B* **833** (2022) 137341, [[2205.12210](#)].
- [68] S.-M. Choi, Y.-J. Kang, H. M. Lee and T.-G. Ro, *Lepto-Quark Portal Dark Matter*, *JHEP* **10** (2018) 104, [[1807.06547](#)].
- [69] G. Belanger et al., *Leptoquark manoeuvres in the dark: a simultaneous solution of the dark matter problem and the $R_{D^{(*)}}$ anomalies*, *JHEP* **02** (2022) 042, [[2111.08027](#)].
- [70] K. Chandak, T. Mandal and S. Mitra, *Hunting for scalar leptoquarks with boosted tops and light leptons*, *Phys. Rev. D* **100** (2019) 075019, [[1907.11194](#)].
- [71] A. Bhaskar, T. Mandal and S. Mitra, *Boosting vector leptoquark searches with boosted tops*, *Phys. Rev. D* **101** (2020) 115015, [[2004.01096](#)].
- [72] A. Bhaskar, T. Mandal, S. Mitra and M. Sharma, *Improving third-generation leptoquark searches with combined signals and boosted top quarks*, *Phys. Rev. D* **104** (2021) 075037, [[2106.07605](#)].
- [73] ATLAS collaboration, G. Aad et al., *Search for leptoquark pair production decaying into $te^- \bar{t}e^+$ or $t\mu^- \bar{t}\mu^+$ in multi-lepton final states in pp collisions at $\sqrt{s} = 13$ TeV with the ATLAS detector*, *Eur. Phys. J. C* **84** (2024) 818, [[2306.17642](#)].
- [74] H. Al Ali et al., *The muon Smasher’s guide*, *Rept. Prog. Phys.* **85** (2022) 084201, [[2103.14043](#)].
- [75] *Technical Design Report for the Muon Forward Tracker*, tech. rep., 2015.
- [76] N. Ghosh, S. K. Rai and T. Samui, *Search for a leptoquark and vector-like lepton in a muon collider*, *Nucl. Phys. B* **1004** (2024) 116564, [[2309.07583](#)].
- [77] P. Bandyopadhyay, A. Karan, R. Mandal and S. Parashar, *Distinguishing signatures of scalar leptoquarks at hadron and muon colliders*, *Eur. Phys. J. C* **82** (2022) 916, [[2108.06506](#)].
- [78] I. Doršner, S. Fajfer, A. Greljo, J. F. Kamenik and N. Košnik, *Physics of leptoquarks in precision experiments and at particle colliders*, *Phys. Rept.* **641** (2016) 1–68, [[1603.04993](#)].
- [79] A. Alloul, N. D. Christensen, C. Degrande, C. Duhr and B. Fuks, *FeynRules 2.0 - A complete toolbox for tree-level phenomenology*, *Comput. Phys. Commun.* **185** (2014) 2250–2300, [[1310.1921](#)].
- [80] J. Alwall, R. Frederix, S. Frixione, V. Hirschi, F. Maltoni, O. Mattelaer et al., *The automated computation of tree-level and next-to-leading order differential cross sections, and their matching to parton shower simulations*, *JHEP* **07** (2014) 079, [[1405.0301](#)].
- [81] T. Sjostrand, S. Mrenna and P. Z. Skands, *PYTHIA 6.4 Physics and Manual*, *JHEP* **05** (2006) 026, [[hep-ph/0603175](#)].
- [82] DELPHES 3 collaboration, J. de Favereau, C. Delaere, P. Demin, A. Giammanco, V. Lemaître, A. Mertens et al., *DELPHES 3, A modular framework for fast simulation of a generic collider experiment*, *JHEP* **02** (2014) 057, [[1307.6346](#)].
- [83] Y. L. Dokshitzer, G. D. Leder, S. Moretti and B. R. Webber, *Better jet clustering algorithms*, *JHEP* **08** (1997) 001, [[hep-ph/9707323](#)].
- [84] M. Cacciari, G. P. Salam and G. Soyez, *FastJet User Manual*, *Eur. Phys. J. C* **72** (2012) 1896, [[1111.6097](#)].
- [85] G. Cowan, K. Cranmer, E. Gross and O. Vitells, *Asymptotic formulae for likelihood-based tests of new physics*, *Eur. Phys. J. C* **71** (2011) 1554, [[1007.1727](#)]. [Erratum: *Eur. Phys. J. C* **73**, 2501 (2013)].